Publisher: GSA
Journal: GEOL: Geology
DOI:10.1130/G37144.1

Controls on transgressive sill growth

Richard J. Walker

Department of Geology, University of Leicester, University Road, Leicester LE1 7RH, UK

ABSTRACT

Igneous sills represent an important contribution to upper crustal magma transport and storage. This study focuses on an exemplary 20–50-m-thick transgressive sill in the Faroe Islands, on the European Atlantic passive margin, which is hosted in layered lavas (1–20 m thick) and basaltic volcaniclastic units (1–30 m thick). Preserved steps in the sill, and offset intrusive segments, are consistent with initial propagation as segmented fractures, followed by inflation to create a through-going sheet. Although steps correspond to the position of some host rock interfaces and volcaniclastic horizons, most interfaces are bypassed. Transgressive sill contacts are sub-parallel to thrust faults that record ENE-WSW shortening, which are observed within the surrounding country rock, and within the sill. Remnant sill segments are elongate along a NNW-SSE axis, parallel to the derived intermediate stress axis for thrust faults. The overall transgressive geometry is consistent with regional horizontal shortening, with steps indicating transitions between transgressive and lateral sill propagation controlled locally by layering. This work emphasizes the importance of scale of observation in considering the controls on sill emplacement, and in particular, that layering is not the primary control on geometry.

INTRODUCTION

Igneous sills represent an important contribution to upper crustal magma transport (e.g., Airoldi et al., 2011; Muirhead et al., 2014), acting as magma conduits and stores. Sill emplacement in basin settings can impact subsurface fluid flow (e.g., water aquifer and hydrocarbon systems: Gudmundsson and Løtveit, 2012), and the maturation of hydrocarbons (Malthe-Sørenssen et al., 2004). Large volumes of transgressive, *saucer-shaped* sills are identified in three-dimensional (3-D) seismic data sets across basin systems (e.g., Thomson and Hutton, 2004), and show that individual sills comprise a series of lobes that record phases of sill propagation. Field-based observations of saucer-shaped sills (e.g., Polteau et al., 2008; Schofield et al., 2010, 2012), indicate that these lobes may also comprise smaller structures, such as segmented elongate fingers, which record phases of inflation and linkage during intrusion. Both observation scales have invoked the role of host rock strength in controlling sill geometry, but it should be noted that 3-D seismic resolution is too low to make this critical correlation. This paper highlights stress controls on transgressive sill emplacement, exemplified in the Faroe Islands (Fig. 1; Fig. DR1 in the GSA Data Repository[1]), on the European Atlantic margin. Detailed mapping shows that the Streymoy sill (Fig. 1) intruded as segmented fractures, which inflated and linked to create a stepped, through-going sheet. Overall geometry is controlled by regional stress, with local propagation controlled by layering, but there is no strict relationship between sill steps and “weak” units or layer interfaces. These observations have direct importance to transgressive sills identified in volcanic sub-systems, and particularly studies that infer major effects of intrusion, on host rock properties or maturation (e.g., Svensen et al., 2004).

FAROE ISLANDS TRANSGRESSIVE SILLS

The Faroe Islands host several transgressive sills that intrude near-horizontal (0–3° dip) basaltic lavas and volcaniclastic units of the Palaeocene-age Malinstindur, Sneis, and Enni Formations (oldest to youngest; Fig. 2). The Malinstindur Formation is dominated by 1–3-m-thick compound basalt lavas that are commonly separated by volcaniclastic sandstone units (<2 m thick), but which account for <10% of the sequence where studied. The Sneis Formation is entirely volcaniclastic, ranging from sandstones to conglomerates, with a total thickness ranging from 1 to 30 m (Passey and Jolley, 2008). The Enni Formation comprises interbedded simple (~2–20-m-thick) and compound (~1–3-m-thick) lavas, and <2-m-thick volcaniclastic sandstone units. Fault and fracture characterization through this sequence (Walker et al., 2013) shows that strain is accommodated through initial brittle failure in lavas, and ductile flow within volcaniclastic sandstone units, highlighting contrasting mechanical properties within the sequence. This paper focuses on the Streymoy sill (see e.g., Hansen et al., 2011), which covers ~17 km^2, with a vertical extent of ~480 m. Hansen et al. (2011) separated the sill into two broad 'saucer' shapes, which were referred to as the northwest and southeast segments (Fig. 1A). Thickness ranges from 20 to 30 m in the northwest segment, and 40–50 m in the southeast segment. The estimated pre-erosion volume is ~2 km^3 (Hansen et al. 2011). Erosion has resulted in variable incision through the stratigraphy, and the sills can be identified in the topography by roches moutonées (Fig. 2B). Mapping of the top and bottom sill contacts, and inclined sheets associated with the sill, where this style of erosion has not occurred, shows that roches moutonées are parallel to steps in the sill, and are estimated to be within ~1 m of the original sill contact.

INTRUSION GEOMETRY

The Streymoy sill southeast segment shows evidence of a ‘saucer-shaped’ geometry, displaying a flat inner region and a transgressive periphery, which locally dips ≤35° (e.g., Figures 1B and 2A). As shown in Figure 2, however, closer inspection of the sill reveals that it transgresses as a series of inclined sections (dipping 7–35°), which are separated by flat sections (dipping 0–3°). Flat sections have lateral extents (parallel to dip) of ~300–350 m where observed (e.g., Figures 2A and 2C). Inclined sections accommodate a range of transgression scales, from ~60 m (e.g., Fig. 2B), to ~250 m (e.g., Figures 2A and 2B) measured parallel to dip. Sill contacts on transgressive sections display regular undulations (Figs. 2C and 3), with the top contact showing consistent wavelengths of ~40–60 m and amplitudes ranging from 5 to 25 m, and bottom contacts showing a stepped geometry at the same scale (Figs. 2B, 2C, and 3C). Individual steps in the basal contact cannot be measured, but top contact steps in the form of roches moutonées are continuous for 220–310 m laterally (Fig. 1).

Although flat sections of individual steps correspond to some lava unit interfaces or volcaniclastic units, including those of the Sneis Formation (Fig. 2), individual sill steps transect most units and unit interfaces. It is important to note also that overall, the sill ‘flat’ sections dip at 0–3°W, whereas host units in the study area, dip 2–3°E, so “flat” sections of the sill are still mildly transgressive through the stratigraphy. For example, the large sill flat sections correspond locally to the position of the volcaniclastic Sneis Formation, but the lowermost part of the flat occurs ~10–20 m stratigraphically below it, within Malinstindur Formation lavas (Fig. 2B).

The sill and host rock are cut by a network of conjugate northeast- and southwest-dipping, millimeter-to-centimeter displacement, calcite- and zeolite-mineralized thrust

DOI:10.1130/G37144.1

faults that dip sub-parallel to the inclined sections of the sill (Figs. 2A and 2C), however, it is noted that steps do not correspond to the position of thrusts, nor do the thrusts accommodate sufficient displacement to account for the scale of the steps. Thrusts dip in the range 20–40°SW, and 5–30°NE. Walker et al. (2011) showed that those thrust faults accommodated ENE-WSW to northeast-southwest contraction (see Figure 2C inset), and are associated with strike-slip faults that accommodate an east-west contraction, and north-south extension (see Figure 2B inset). The sills cut conjugate dikes that also accommodate east-west contraction and north-south extension, indicating that the sills were emplaced during a regional east-west compression. Calculated palaeostress axes (e.g., Figures 2B and 2C insets) correlate well with sill geometry in that (1) sill contacts are sub-parallel to conjugate thrust faults, and form an acute angle to the calculated σ_1-σ_2 plane for those thrusts (e.g., Fig. 2C), and (2) relict sill segments are elongate parallel to the calculated σ_2 axis for conjugate thrust faults (NNW-SSE).

Steps observed on the contacts of the Streymoy sill (e.g., Fig. 3B) are consistent with step features observed in dikes (e.g., Pollard et al., 1975), sills (e.g., Schofield et al., 2012), and echelon joint and vein sets (e.g., Pollard et al., 1982). In such cases, steps are shown to result from linkage of offset or en echelon intrusion or fracture segments, which coalesce to a single sheet. Segmented sill-parallel minor intrusions (Fig. 3a), and sill internal contacts (Figs. 2A and 3C), are inferred here to record the early stages of intrusion as segments, ahead of a through-going sheet.

CONTROLS ON TRANSGRESSIVE SILL GEOMETRY

Numerical models for centrally-fed sills emplaced into isotropic elastic media (e.g., Malthe-Sørenssen et al., 2004), and analogue models for intrusion using homogenous media (e.g., Galland et al., 2009) indicate that transgressive 'saucer-shaped' sills are a fundamental shape in shallow systems. Malthe-Sørenssen et al. (2004) showed that the development of a saucer shape, from an established flat sill, is strongly controlled by stress asymmetry ahead of the propagating crack tip: the sill would propagate as a flat intrusion until it had spread to a radius approximately equal to the depth of emplacement, when doming in the overburden would affect a tensile stress asymmetry ahead of the tip, leading to upward propagation. These experiments were conducted using isotropic media, which indicates transgression is controlled by overburden deformation, rather than host mechanical layering. This point is supported by observations of the Streymoy sill. For instance, the broad 'flat' part of the sill shown in Figure 2C, does not directly exploit the Sneis Formation contacts. The implication is that although the layered host sequence may promote horizontal propagation of the sill, that layering plays a secondary (albeit locally important) role in the overall sill geometry.

Steps observed in the Streymoy sill contacts, and in minor sheets adjacent to the sill (e.g., Fig. 3A), are interpreted to represent sill propagation as a series of segmented fractures, which inflated and linked to create a through-going sheet. Studies of fracture and fault propagation in elastic multilayers (e.g., Schöpfer et al., 2006; Walker at al., 2013) have shown that during regional extension, fractures develop initially in the mechanically "stronger" (brittle) units, before linking through "weaker" (ductile) units as strain increases. Walker et al. (2013) showed that faults cutting interlayered (basaltic) volcaniclastic-lava sequences develop initially through brittle failure in the lava, and ductile flow within volcaniclastic units. The result of this early-developed fracture architecture is that the through-going faults display significant steps. A similar effect could occur during regional compression, with fractures developing sub-horizontally rather than sub-vertically. Layer-bound fracturing could also lead to fractures propagating preferentially in (NNW-SSE horizontal) the σ_2 axis, rather than growing in the (southeast-plunging) σ_1 axis, as a result of individual fractures being impeded by existing discontinuities. Transgressive steps in the sill occur at the meter to tens of meters scale, associated with thin-unit boundaries (e.g., 1–3-m-thick compound lavas and sediments: Fig. 3A), and at the hundred-meter scale, associated with thick-unit boundaries (e.g., the Sneis Formation: Fig. 2C). The implication here is that the sill intruded as cracks that inflated to form a through-going sheet, but that vertical propagation of individual segments was locally impeded by mechanical contrasts (such as strength, Poisson's ratio, and Young's modulus) in the host sequence (Fig. 4). Sill steps may therefore preserve the initial strain gradient from a through-going portion of the transgressive sill, with NNW-SSE horizontal intrusion and inflation only possible once cracks becomes connected to the source. Host mechanical properties therefore play an important role in the local propagation and segmentation of the sill, either in focusing propagation (e.g., along unit interfaces), or by impeding propagation across mechanical layers or discontinuities, but the overall geometry is a record of the northeast-southwest compression.

AN ALTERNATIVE MODEL FOR TRANSGRESSIVE SILL EMPLACEMENT

The transgressive geometry of the Streymoy sill, combined with evidence for local mechanical control in the early development of the sill as segments, is consistent with the development of a shallowly-dipping hydrofracture system, similar to that described by Baer (1995). In that model, intrusion by brittle fracture involved phases of fracture propagation ahead of the leading edge of the magma, followed by tip fluid propagation, and conduit flow. I infer here that emplacement of the Streymoy sill can be summarized into four stages (Fig. 4):

(1) Regional ENE-WSW contraction and NNW-SSE extension, coupled with magmatic pressure-driven failure in the host rock, facilitated horizontal propagation of a flat elliptical sill (Fig. 4A), sub-parallel with the σ_1-σ_2 plane (i.e., gently WSW-dipping) related to regional horizontal shortening.

(2) As the radius of the elliptical sill reached a value approximately equal to the depth of emplacement, doming of the overburden resulted in asymmetric tensile stress ahead of the propagating sill tip, facilitating an upward deflection (Fig. 4B).

(3) Host mechanical layering resulted in preferential fracture and fault development in elastically compliant layers (i.e., layers with a lower resistance to fracture), leading to NNW-SSE layer-bound fracture propagation parallel to σ_2 (Figs. 4C and 4Di).

(4) As strain increased through inflation, transgressive fracture tips linked individual sill segments to create a through-going sill (Figs. 4Dii and 4Diii).

It is important to note that "layering" in this case, may refer to sequences of units, such as multiple lavas, rather than individual units. As with studies in fault systems (e.g,, Schöpfer et al., 2006) the extent of individual segments (as measured in the dip direction) during initial sill propagation is related to the thickness of the host layering and reflects the distribution of existing fractures in the host rock (Fig. 4C). Upward propagation in stage 2 could lead to a reduction in magma pressure and flexural strain at the sill periphery (Malthe-Sørenssen et al., 2004). This would promote magma propagation as flat-lying sills that preferentially exploit bedding planes (e.g., Fig. 4D). This type of effect has been proposed elsewhere in discussion of flat outer rims on sills (e.g., Goulty and Schofield, 2008; Airoldi et al., 2011). Flat zones are observed in the Streymoy sill at various elevations (e.g., Figures 2A and 2B), which may be explained by this mechanism, but it is noted that flat sections of the sill cut through a number of unit interfaces, including the formation boundary between the Malinstindur Formation compound lavas, and the sedimentary Sneis Formation.

CONCLUSIONS

The Streymoy sill is an exemplary transgressive sill formed during horizontal shortening. Although the sill is hosted in mechanically layered units, the broad geometry is consistent with models for emplacement in an isotropic medium. Steps indicate that mechanical layering is important in controlling local propagation and contact geometry, which is important when considering processes associated with transport and storage of magma in the subsurface. Notably, major sedimentary horizons in the lava-dominated sequence are not preferentially intruded, but still impose geometric controls on the sill. The mechanical contrast here is comparable to sandstone-mudstone sequences, in which sandstones represent the stronger material. Most steps are below seismic imaging scales, emphasizing the importance of the scale of observation in understanding intrusion emplacement controls and mechanisms.

ACKNOWLEDGMENTS

Observations crucial to this study were made during Walker’s Ph.D. research, which was funded by Statoil (UK) Ltd. Thanks to Ken McCaffrey, Bob Holdsworth, and Richard England, and Nick Schofield and the anonymous reviewers for very detailed reviews that greatly benefit the paper. Thanks to the Føroya Dàtusavn for access to aerial imagery.

REFERENCES CITED

Airoldi, G., Muirhead, J.D., White, J.D.L., and Rowland, J.V., 2011, Emplacement of magma at shallow depth: insights from field relationships at Allan Hills, south Victoria Land, East Antarctica: Antarctic Science, v. 23, p. 281–296, doi:10.1017/S0954102011000095.

Baer, G., 1995, Fracture propagation and magma flow in segmented dykes: Field evidence and fabric analysis, Makhtesh Ramon, Israel, *in* Baer, G., and Heinmann, A.A., eds., Physics and Chemistry of Dykes: Rotterdam, Netherlands, A.A. Balkema, p. 125–140.

Galland, O., Planke, S., Neumann, E.R., and Malthe-Sørenssen, A., 2009, Experimental modelling of shallow magma emplacement: Application to saucer-shaped intrusions: Earth and Planetary Science Letters, v. 277, p. 373–383, doi:10.1016/j.epsl.2008.11.003.

Goulty, N., and Schofield, N., 2008, Implications of simple flexure theory for the formation of saucer-shaped sills: Journal of Structural Geology, v. 30, p. 812–817, doi:10.1016/j.jsg.2008.04.002.

Gudmundsson, A., and Løtveit, I.F., 2012, Sills as fractured hydrocarbon reservoirs: Examples and models, *in* Spence, G.H., et al., eds., Advances in the Study of Fractured Reservoirs: Geological Society of London Special Publication 374, p. 251–271.

Hansen, J., Jerram, D.A., McCaffrey, K.J.W., and Passey, S.R., 2011, Early Cenozoic saucer-shaped sills of the Faroe Islands: An example of intrusive styles in basaltic lava piles: Journal of the Geological Society, v. 168, p. 159–178, doi:10.1144/0016-76492010-012.

Malthe-Sørenssen, A., Planke, S., Svensen, H., and Jamtveit, B., 2004, Formation of saucer-shaped sills, *in* BreitKreuz, C., and Petford, N., eds., Physical Geology of High-Level Magmatic Systems: Geological Society of London Special Publication, 234, p. 215–227.

Muirhead, J.D., Airoldi, G., White, J.D.L., and Rowland, J.V., 2014, Cracking the lid: Sill-fed dikes are the likely feeders of flood basalt eruptions: Earth and Planetary Science Letters, v. 406, p. 187–197, doi:10.1016/j.epsl.2014.08.036.

Passey, S.R., and Jolley, D.W., 2008, A revised lithostratigraphic nomenclature for the Palaeogene Faroe Islands Basalt Group, NE Atlantic Ocean: Transactions of the Royal Society of Edinburgh, Earth and Environmental Science, v. 99, p. 127–158, doi:10.1017/S1755691009008044.

Pollard, D.D., Muller, O.H., and Dockstader, D.R., 1975, The form and growth of fingered sheet intrusions: Geological Society of America Bulletin, v. 86, p. 351–363, doi:10.1130/0016-7606(1975)86<351:TFAGOF>2.0.CO;2.

Pollard, D.D., Segall, P., and Delaney, P.T., 1982, Formation and interpretation of dilatant echelon cracks: Geological Society of America Bulletin, v. 93, p. 1291–1303, doi:10.1130/0016-7606(1982)93<1291:FAIODE>2.0.CO;2.

Polteau, S., Ferre, E.C., Planke, S., Neumann, E.-R., and Chevallier, L., 2008, How are saucer-shaped sills emplaced? Constraints from the Golden Valley Sill, South Africa: Journal of Geophysical Research, v. 113, B12104, doi:10.1029/2008JB005620.

Schofield, N., Stevenson, C., and Reston, T., 2010, Magma fingers and host rock fluidization in the emplacement of sills: Geology, v. 38, p. 63–66, doi:10.1130/G30142.1.

Schofield, N., Brown, D.J., Magee, C., and Stevenson, C.T., 2012, Sill morphology and comparison of brittle and non-brittle emplacement mechanisms: Journal of the Geological Society, v. 169, p. 127–141, doi:10.1144/0016-76492011-078.

Schöpfer, M.P.J., Childs, C., and Walsh, J.J., 2006, Localisation of normal faults in multilayer sequences: Journal of Structural Geology, v. 28, p. 816–833, doi:10.1016/j.jsg.2006.02.003.

Sperner, B., Ratschbacher, L., and Ott, R., 1993, Fault-Striae analysis: a Turbo Pascal program package for graphical presentation and reduced stress tensor calculation: Computers & Geosciences, v. 19, p. 1361–1388, doi:10.1016/0098-3004(93)90035-4.

Svensen, H., Planke, S., Malthe-Sørenssen, A., Jamtveit, B., Myklebust, R., Rasmussen Eidem, T., and Rey, S.S., 2004, Release of methane from a volcanic basin as a mechanism for initial Eocene global warming: Nature, v. 429, p. 542–545, doi:10.1038/nature02566.

Thomson, K., and Hutton, D., 2004, Geometry and growth of sill complexes: Insights using 3D seismic from the North Rockall Trough: Bulletin of Volcanology, v. 66, p. 364–375, doi:10.1007/s00445-003-0320-z.

Walker, R.J., Holdsworth, R.E., Imber, J., and Ellis, D., 2011, Onshore evidence for progressive changes in rifting directions during continental break-up in the NE

Atlantic: Journal of the Geological Society, v. 168, p. 27–48, doi:10.1144/0016-76492010-021.

Walker, R.J., Holdsworth, R.E., Imber, J., Faulkner, D.R., and Armitage, P.J., 2013, Fault zone architecture and fluid flow in interlayered basaltic volcaniclastic-crystalline sequences: Journal of Structural Geology, v. 51, p. 92–104, doi:10.1016/j.jsg.2013.03.004.

FIGURE CAPTIONS

Figure 1. The Streymoy Sill, Faroe Islands. A: Aerial image showing the positions and inferred extent of the northwest and southeast segments (after Hansen et al., 2011). B: Hill-shaded topographic image (illuminated from 315) with color-coded elevation for the exposed areas of the sill. C: Aerial image showing color-coded slope (dip) data for the exposed areas of the sill.

Figure 2. Cross sections through the Streymoy sill: view-fields shown in Figure 1C. A: View northwest to the southernmost outcrops of the southeast segment, showing the overall northeast and southwest transgressive nature of the sill. Insets show (i) variable attitudes of joints within the sill, and (ii) stepping basal contact of the sill. Horizontal rock exposures correspond to lava core zones, showing that sill steps do not correspond to individual lava interfaces. B: Northwest segment shows a stepped transgression up to the northeast. Note that the photo perspective means that the left of the image is oriented northeast-southwest, and the right of the image shows northwest-southeast. C: Cross section through the northwest segment of the sill, showing relationship to inclined “feeder” dikes (after Hansen et al., 2011), and thrust faults. Lower hemisphere

stereographic projection insets are for (B) faults within the lava host rock (left) and calculated principal compressive stress axes (where $\sigma_1 > \sigma_2 > \sigma_3$) with the maximum horizontal compression direction (right), and (C) thrust faults (left) and calculated principal stress axes (right). Principal stress attitudes were calculated using the simple shear tensor average method (Sperner et al., 1993). Fmn—Formation.

Figure 3. Intrusion segments, and relict segments. A: Inclined intrusion (see Figure 2C for location) is segmented and discontinuous in this cross section. Segment tips are commonly spatially associated with host unit interfaces, though individual segments also cut a number of host contacts. B: Transgressive and flat parts of the southeast segment show steps at the meter and tens of meter scales. C: Internal contact in the southeast segment (location shown in Fig. 2A). D: Oblique cut-through of a transgressive part of the southeast segment (location indicated in Fig. 1C). Relict segments are elongate northwest-southeast. The sill is accommodated by ~50 m of apparent vertical uplift of the host stratigraphy, whereas the sill thickness measured normal to the margins is ~30 m.

Figure 4. Conceptual model for the propagation of the Streymoy sill. A–C: Maps (left) and cross sections (right). See text for details. A: Flat, elliptical sill emplacement. B: Overburden doming results in upward deflection of the crack tip. C: Transgression and propagation of the sill is controlled locally by mechanical layering. D: Inflation of fractures leads to linkage, forming a through-going sheet. Panels i–iii show the progressive stages of inflation from fractures to a linked sheet.

[1]GSA Data Repository item 2016xxx, xxxxxxxx, is available online at www.geosociety.org/pubs/ft2016.htm, or on request from editing@geosociety.org or Documents Secretary, GSA, P.O. Box 9140, Boulder, CO 80301, USA.

Fig. 1

W: 123 mm
H: 52.6 mm

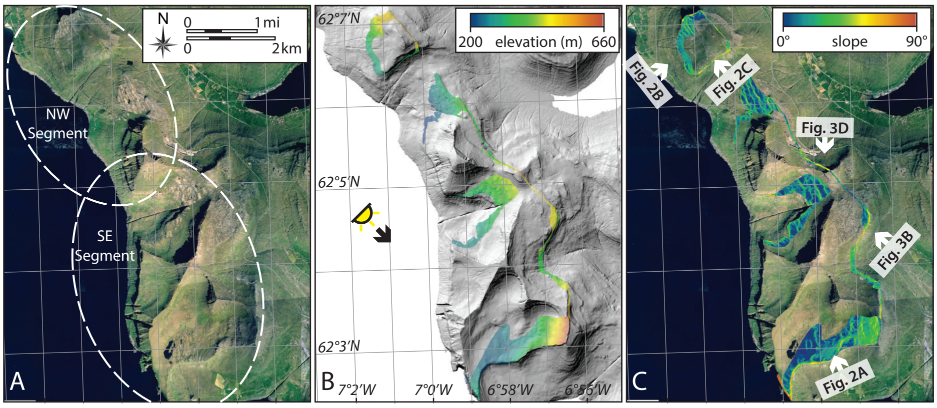

Fig. 2

W: 123 mm
H: 95 mm

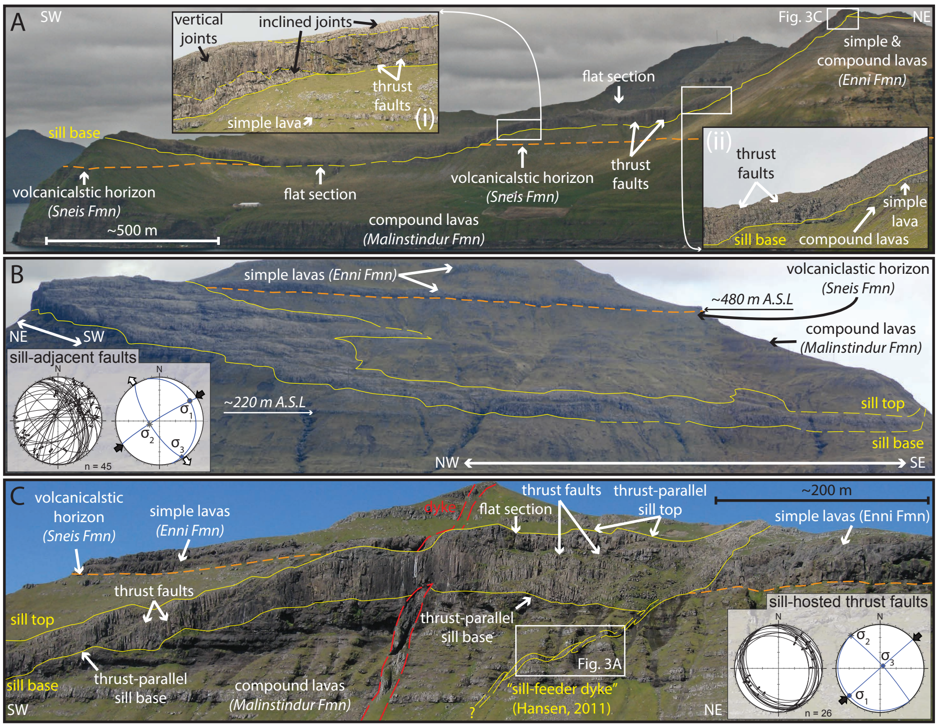

Fig. 3
W: 123 mm
H:106 mm

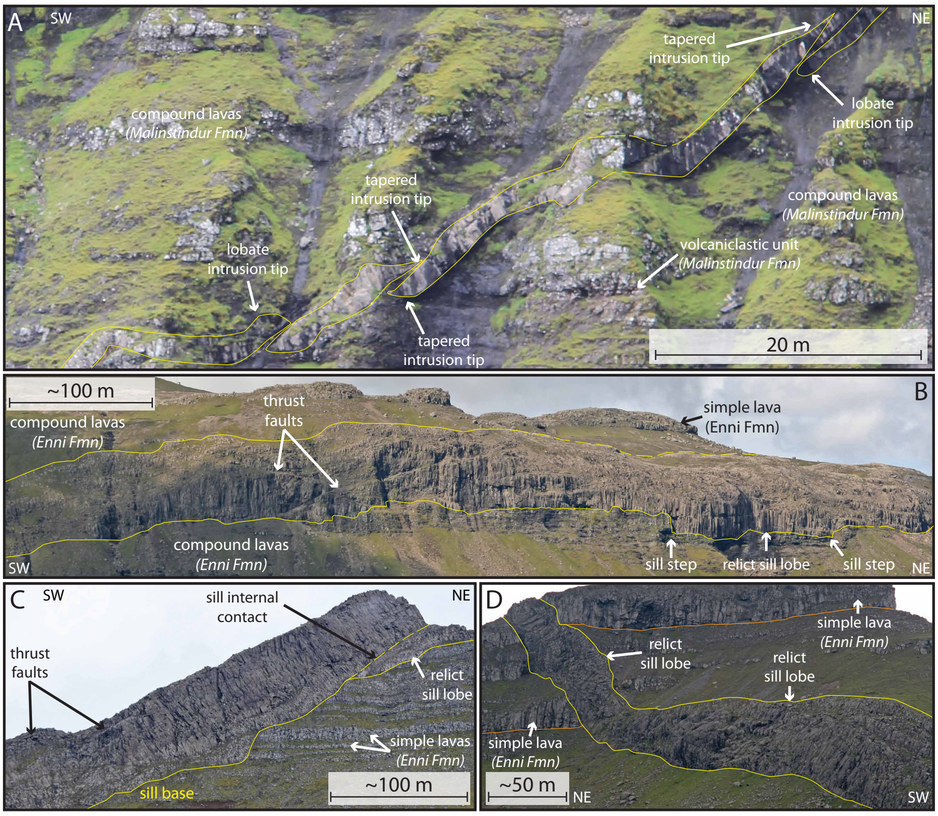

Fig. 4
W: 61 mm
H: 101 mm